Available online at www.sciencedirect.com

SCIENCE DIRECT

Brain Research 1052 (2005) 212 – 221

BRAIN RESEARCH

www.elsevier.com/locate/brainres

Research Report

Lack of the alanine–serine–cysteine transporter 1 causes tremors, seizures, and early postnatal death in mice

Xinmin Xie[a,b,c,*], Theodore Dumas[c], Lamont Tang[a], Thomas Brennan[a], Thadd Reeder[a], Winston Thomas[a], Robert D. Klein[a], Judith Flores[c], Bruce F. O'Hara[c], H. Craig Heller[c], Paul Franken[c]

[a]*Deltagen Inc., San Carlos, CA 94070, USA*
[b]*AfaSci Inc., Burlingame, CA 94010, USA*
[c]*Department of Biological Sciences, Stanford University, Stanford, CA 94305, USA*

Accepted 10 June 2005
Available online 18 July 2005

Abstract

The Na^+-independent alanine–serine–cysteine transporter 1 (Asc-1) is exclusively expressed in neuronal structures throughout the central nervous system (CNS). Asc-1 transports small neutral amino acids with high affinity especially for D-serine and glycine (K_i: 8–12 μM), two endogenous glutamate co-agonists that activate *N*-methyl-D-aspartate (NMDA) receptors through interacting with the strychnine-insensitive glycine binding-site. By regulating D-serine (and possibly glycine) levels in the synaptic cleft, Asc-1 may play an important role in controlling neuronal excitability. We generated *asc-1* gene knockout (*asc-1*$^{-/-}$) mice to test this hypothesis. Behavioral phenotyping combined with electroencephalogram (EEG) recordings revealed that *asc-1*$^{-/-}$ mice developed tremors, ataxia, and seizures that resulted in early postnatal death. Both tremors and seizures were reduced by the NMDA receptor antagonist MK-801. Extracellular recordings from *asc-1*$^{-/-}$ brain slices indicated that the spontaneous seizure activity did not originate in the hippocampus, although, in this region, a relative increase in evoked synaptic responses was observed under nominal Mg^{2+}-free conditions.

Taken together with the known neurochemistry and neuronal distribution of the Asc-1 transporter, these results indicate that the mechanism underlying the behavioral hyperexcitability in mutant mice is likely due to overactivation of NMDA receptors, presumably resulting from elevated extracellular D-serine. Our study provides the first evidence to support the notion that Asc-1 transporter plays a critical role in regulating neuronal excitability, and indicate that the transporter is vital for normal CNS function and essential to postnatal survival of mice.

Theme: Neurotransmitters, modulators, transporters, and receptors
Topic: Excitatory amino acid receptors: physiology, pharmacology and modulation

Keywords: Asc-1 transporter; D-Serine; Knockout; Seizure; Tremor

1. Introduction

Amino acids are normally present as L-forms with the exception of D-serine, D-aspartate, and D-alanine which are found at relatively high concentrations in the CNS [8,10,18,20]. D-serine has been shown to be liberated from glial cells near NMDA receptors [22,23] and can enhance NMDA receptor activation by activating the strychnine-insensitive glycine binding site with an affinity 3- to 4-fold

Abbreviations: Asc-1, Na^+-independent alanine–serine–cysteine transporter 1; *asc-1*, the gene encoding Asc-1; ASCT1 and -2, Na^+-dependent alanine–serine–cysteine transporter 1 and 2; ES, embryonic stem cells; FP, fiber potential; GlyT-1 and -2, glycine specific transporter-1 and -2; I/O, input/output; IRES-*lacZ*-neo, IRES-*lacZ* reporter and neomycin resistance cassette; KO, knockout; NMDA, *N*-methyl-D-aspartate; PS, population spikes; WT, wild-type

* Corresponding author. AfaSci Inc., Burlingame, CA 94010, USA. Fax: +1 650 692 6051.
E-mail address: simonxie@afasci.com (X. Xie).

0006-8993/$ - see front matter © 2005 Elsevier B.V. All rights reserved.
doi:10.1016/j.brainres.2005.06.039

larger than glycine itself [13,23]. Overactivation of NMDA receptors has been implicated in several pathological conditions, such as seizures and neurodegenerative disorders [15]. Maintenance of appropriate extracellular concentrations of D-serine and glycine in the CNS may be critical in controlling NMDA receptor activation. Regulation of D-serine and glycine levels, in turn, depends on several mechanisms. In addition to D-serine synthesis, involving serine racemase, extracellular D-serine levels depend on the activity of D-serine metabolizing enzymes such as D-amino acid oxidase and uptake through specific transporters [9].

Two Na^+-dependent alanine–serine–cysteine transporters (ASCT1 and -2) have been identified, but these two transporters have lower affinities (K_i: 29–88 μM) for D-amino acids compared to L-amino acids [1,21,26]. More recently, a Na^+-independent alanine–serine–cysteine transporter termed Asc-1 (or *Slc7a10*: solute carrier family 7, cationic amino acid, transporter, y+ system, member 10) has been cloned and characterized, which has a high affinity for small neutral amino acids in particular for D-serine and glycine (K_i: 8–13 μM) [5,14,16]. Basal extracellular levels of D-serine which were estimated to be around 6.5 μM in rat prefrontal cortex and striatum, could reach the transporter's affinity, especially in the synaptic cleft during excitatory neuronal activity [9,10]. In contrast to the ASCT1 and ASCT2 transporters, Asc-1 shows no apparent stereoselectivity between L- and D-amino acids [11]. A second member of this transporter gene family, Asc-2, is more selective for L- than D-serine [2].

Asc-1 has a widespread distribution in the CNS and is present exclusively in neuronal structures such as nerve cell bodies and dendritic fields, whereas both glia and white matter are devoid of Asc-1. At the ultrastructural level, Asc-1 is confined mainly to presynaptic terminals and dendrites of principal neurons in the cortex, hippocampus, and cerebellum [11,14]. In contrast, Asc-2 is predominantly expressed in peripheral tissues, e.g., kidney, and was not detected in the brain tissue [2]. For these reasons, it has been hypothesized that Asc-1 could be critical in regulating extracellular D-serine levels and may specifically contribute to synaptic clearance of D-serine in the CNS [5,11]. A physiological role of Asc-1 has, however, not been demonstrated, in part due to the lack of selective inhibitors for this transporter. In the present study, we have taken the gene-targeted deletion, i.e., knockout (KO) approach and employed basic behavioral phenotypic and electrophysiological analyses to address this fundamental question. Preliminary results were communicated in abstract form [25].

2. Materials and methods

2.1. Generation of *asc-1*$^{-/-}$ mice

Using conventional transgenic and mouse breeding techniques as described previously [17], a genomic fragment of about 6.0 kb, including Asc-1 protein-coding regions of the *asc-1* gene, was isolated from a mouse genomic library and subcloned into the *Bam*HI site of the pBluescript II SK(−) vector. A 115-bp fragment corresponding to a segment of the protein-coding region was replaced by an IRES-*lacZ* reporter and neomycin (G418) resistance cassette (IRES-*lacZ*-neo; Fig. 1). This mutation was designed to produce a loss-of-function mutation by

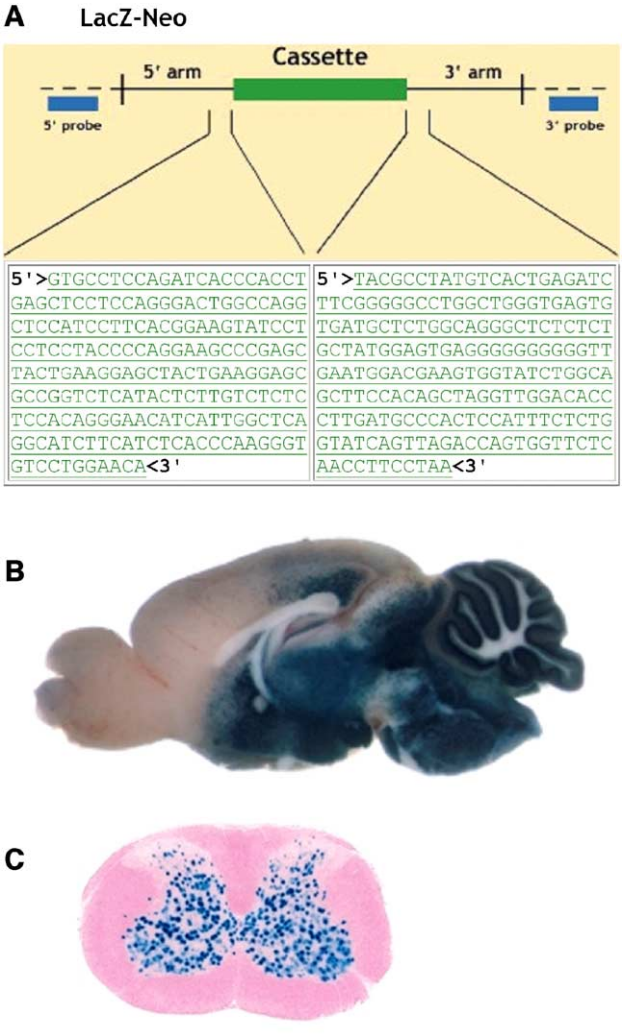

Fig. 1. Structure of the *asc-1* targeting vector and *lacZ* expression analysis. (A) Illustration of the structure of the *asc-1* targeting vector with respect to the genomic locus. The dashed lines indicate genomic DNA which lies outside of the targeting vector. The 5′ arm is approximately 3.5 kb and the 3′ arm is approximately 2.5 kb. The genomic DNA sequence which lies adjacent to the 5′ and 3′ aspects of the *lacZ*-neo cassette is indicated below the construct diagram. The 5′ (GCTGTCAGTCAGATGGTCACCTAAG) and 3′ (GTCTCAGCTCTTCAAAGTGTCCTTGG) probes used for PCR analysis of homologous recombinants are indicated in blue. (B) *LacZ* staining (in blue) indicates *lacZ* expression in the sagittal brain section taken from a 7-week-old heterozygous mutant mouse. The *lacZ* is heterogeneously expressed in the brain with highest staining in the brainstem, midbrain, diencephalon, and cerebellum. (C) In the spinal cord, substantial *lacZ* staining was present in the gray matter exclusively.

deletion of amino acids 74 to 112, as well as insertion of the 6.9-kb reporter/resistance cassette. The IRES-*lacZ*-neo cassette was flanked by 3.5 kb of mouse genomic DNA at its 5′ aspect and 2.5 kb of mouse genomic DNA at its 3′ aspect. The targeting vector was linearized and electroporated into 129P2/OlaHsd mouse embryonic stem (ES) cells. ES cells were selected for G418 resistance and colonies carrying the homologously integrated IRES-*lacZ*-neo DNA were identified by PCR amplification with neo-specific primers paired with primers located outside the targeting homology arms on both the 5′ and 3′ sides. Colonies that gave rise to the correct size PCR product were confirmed by Southern blot analysis using a probe adjacent to the 5′ region of homology. The presence of a single IRES-*lacZ*-neo cassette was confirmed by Southern blot analysis using a neo gene fragment as a probe.

Male chimeric mice were generated by injection of the targeted ES cells into C57Bl/6 blastocysts. Chimeric mice were bred with C57Bl/6 mice to produce F1 heterozygotes (*asc-1*$^{+/-}$). Germline transmission was confirmed by PCR analysis. F1 heterozygous males and females were mated to produce the F2 wild-type (WT or *asc-1*$^{+/+}$) and homozygous (*asc-1*$^{-/-}$) mutant animals used in this study.

The *lacZ* expression analysis of tissues was taken from 7-week-old heterozygous mutant mice. The brains were frozen, sectioned (10 μm), stained, and analyzed for *lacZ* expression using X-gal as a substrate for β-galactosidase, followed by a Nuclear Fast Red counterstaining.

2.2. Behavioral observation and open-field test

General mouse behavior was closely observed by trained personnel and recorded by a digital camera as appropriate. For the open-field test [3], each animal was placed in the center of the open chamber constructed of opaque PVC, 43 (W) × 43 (D) × 30 (H) cm (SD Instruments, San Diego). Test duration was 10 min with the experimenter out of the animals' sight. Movement of individual mice was detected by photobeam breaks in the *x*, *y*, and *z* axes and recorded for the duration of the test. Measurements taken include total distance traveled and average velocity during the ambulatory episodes, and percent of session time spent in the central or peripheral regions of the test apparatus.

2.3. In vivo electrophysiology

Methods concerning EEG and EMG surgeries, recordings, and analysis are detailed in Franken et al. [4]. Briefly, EEG and EMG electrodes were implanted in WT and KO mice (both sexes, 30–35 days old,) under deep sodium-pentobarbital anesthesia (70 mg/kg, i.p.). Two gold-plated miniature screws served as EEG electrodes and were screwed through the skull over the right cerebral hemisphere. Two semi-rigid gold wires served as EMG electrodes and were inserted along the skull into the neck muscles. The electrodes, which were soldered to a connector plug, were cemented to the skull with dental acrylic. Mice were maintained in poly-carbonate recording cages (31 × 18 × 18 cm) with food and water ad libitum, on a 12-h light–12-h dark cycle (light from 09:00 to 21:00 h), and an ambient temperature between 24.5 and 25.5 °C. After surgery, animals were connected to counterbalanced recording cables allowing the recording of EEG and EMG in freely behaving animals. EEG and EMG signals were recorded continuously starting 1 week after surgery and up to 5 days. The analog EEG and EMG signals were directly AD-converted at 2000 Hz and then down-sampled and stored at 200 Hz on hard disk. Off-line, both signals were subjected to discrete-Fourier transformation (DFT) analysis yielding power spectra between 0 and 90 Hz for selected 4-s epochs. Hardware (EMBLA™) and software (Somnologica-3™) were purchased from Flaga hf. Medical devices (now Medcare, Iceland).

2.4. In vitro electrophysiology

Mice (WT and KO, 30–35 days old) were anesthetized with halothane, decapitated, and their brains were placed into ice-cold oxygenated (95% O_2, 5% CO_2) artificial-cerebrospinal fluid (ACSF in mM: NaCl 125, KCl 3, $MgCl_2$ 2.0, $CaCl_2$ 2.0, $NaHPO_4$ 1.25, $NaHCO_3$ 26, and dextrose 13; pH 7.4). The hippocampus was dissected and sliced parallel to the alvear fibers as previously described [24]. Slices (~400 μm thick) were transferred to an interface recording chamber (at room temperature) to incubate for 1–2 h before recordings. Slices from WT and KO littermates were prepared on the same day and recorded in a counter-balanced fashion. Synaptic responses were elicited in area CA1. The recording electrode was a glass micropipette (2–6 MΩ tip resistance) positioned in stratum radiatum 1 mm from the stimulating electrode (teflon-coated platinum–iridium). In this configuration, the fiber potential (FP) and excitatory postsynaptic potential (EPSP) appear as negative deflections. For population spike (PS) recording, the glass pipette was moved to the stratum pyramidale. In this location, the EPSP is a positive-going wave and the PS is a sharp negative spike superimposed on the EPSP. At each location, 5 responses evoked by each stimulation intensity were recorded to construct input/output (I/O) curves. When recording in normal ACSF was complete, the Mg^{2+} concentration was reduced to 0 mM and, following a 20-min incubation period, I/O curves were recorded a second time in stratum pyramidale. Electrophysiological data were present in mean ± SEM. Two-way repeated-measures analyses of variance (rANOVA) were used to compare I/O curves. For excitability analysis, PS amplitudes were compared by two-way rANOVA with responses collapsed across stimulation level and Mg^{2+} concentration as the repeated measure.

All animal experimental protocols and procedures were approved by the Animal Care and Use Committees of both Deltagen and Stanford University. All chemicals and drugs used in this study were purchased from Sigma and Tocris.

3. Results

3.1. Generation of homozygous asc-1$^{-/-}$ mutant mice

To explore the physiological role of Asc-1, the *asc-1* gene was targeted by homologous recombination and an F1 generation of mice heterozygous for the targeted null allele (*asc-1*$^{+/-}$) was produced (Fig. 1A). The *asc-1*$^{+/-}$ mice appeared phenotypically normal and showed undisturbed development and fertility. F1 mice were intercrossed to generate WT (*asc-1*$^{+/+}$) and homozygous (*asc-1*$^{-/-}$) mice. Expression levels of the reporter gene *lacZ* in *asc-1*$^{+/-}$ mice were heterogeneously distributed throughout the CNS, with highest expression in the thalamus, hypothalamus, brainstem, and cerebellum, lower density in the cortex, and lowest expression in apparent white matter structures (Fig. 1B). Notably, in the spinal cord, *lacZ* was expressed in gray matter exclusively (Fig. 1C).

3.2. Homozygous mutant mice show tremors, ataxia, seizures, and early postnatal death

Although the general appearance of *asc-1*$^{-/-}$ pups seemed normal at birth, body, brain, and other key organs weighted 20–30% less in both male and female mice compared to WT littermate controls as measured on postnatal day 14 (n = 8 for each genotypic group). In contrast to *asc-1*$^{+/+}$ mice, all *asc-1*$^{-/-}$ mice (at age of 20–30 days) appeared runted, assumed a hunched posture, and moved in ataxic gait. In open-field tests, *asc-1*$^{-/-}$ mice exhibited less locomotor activity manifested by a 58 ± 11% reduction in traveling distance (Fig. 2A) and decrease in average velocity, and spent 37 ± 12% more time in peripheral regions compared to *asc-1*$^{+/+}$ mice (Fig. 2B; n = 8 per genotypic group). More obviously, *asc-1*$^{-/-}$ mice displayed periodic spontaneous tremors, tonic–clonic, and seizure-like activities. The tonic–clonic-like activity of *asc-1*$^{-/-}$ mice was manifest as sudden, brief activity bursts lasting for approximately 0.5–1 s and frequently occurred every 2–30 min. Tonic–clonic-like activity often led to hind limb extension or generalized convulsive seizure-like movements lasting for 3–30 s. Between tonic–clonic-like or seizure activities, animals displayed long-lasting tremors. These behavioral abnormalities could be triggered or exacerbated by cage movements, gently tossing of the animal, or sudden acoustic stimuli (similar to startle responses), but were not affected by changes in ambient temperatures (between 18 and 38 °C). In contrast, the frequency of both tonic–clonic-like activity and generalized seizures decreased by 61 ± 2% (Fig. 2C) and tremors were also reduced with the NMDA receptor antagonist MK-801 over the 1-h period following the injection (3 mg/kg, i.p., n = 3) compared to the number of those events occurring following saline injection in the same animals. These results indicate the involvement of the activation of the NMDA receptors. Moreover, the gamma-aminobutyric acid

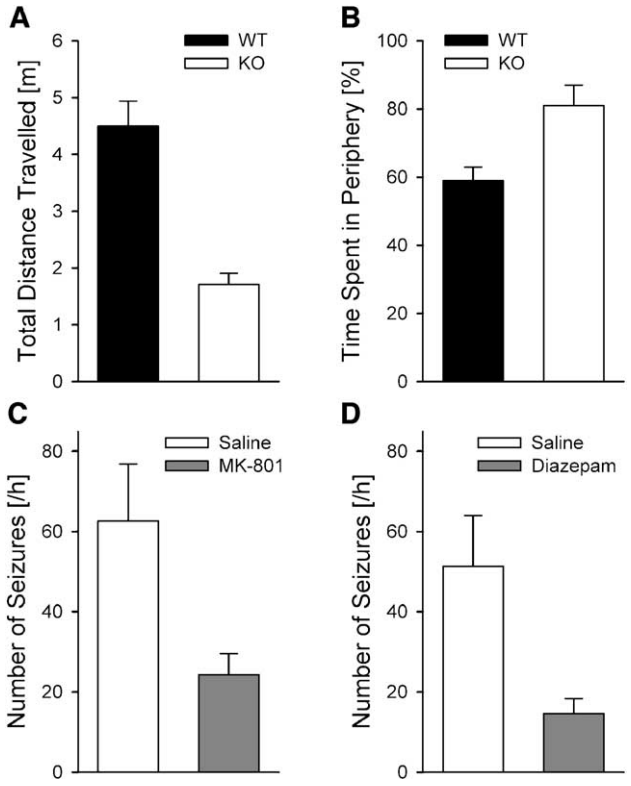

Fig. 2. Neurobehavioral abnormalities of *asc-1*$^{-/-}$ mice were assessed using an open-field test and homecage observations. Data points and bars indicate mean ± SEM. (A) In the open-field test, *asc-1*$^{-/-}$ mice displayed substantial less locomotor activity as measured by total distance traveled compared to WT mice. (B) *asc-1*$^{-/-}$ mice spent a larger percent of session time in the peripheral regions of the test apparatus (A and B: $P < 0.05$, unpaired t tests, n = 8/genotype). (C) The frequency of both tonic–clonic-like activity and generalized seizures was reduced by the treatment of NMDA receptor antagonist MK-801 (3 mg/kg, i.p.). (D) The $GABA_A$ receptor modulator diazepam (10 mg/kg, i.p.) also depressed tonic–clonic-like activity and generalized seizures. In both cases, abnormal behavioral events were counted in the first hour following the injection of either saline or drugs in the same animals (C and D: $P < 0.05$, paired t test, n = 3).

$(GABA)_A$ receptor modulator diazepam, at a high dose of 10 mg/kg (i.p., n = 3), was also capable of temporarily depressing tonic–clonic-like activity and generalized seizures (71 ± 3%; Fig. 2D), suggesting that GABAergic neurotransmission is intact and augmentation of the inhibitory system can overcome neuronal excitability. Most *asc-1*$^{-/-}$ mice did not survive to weaning age (n = 20/26), whereas none of heterozygous *asc*$^{+/-}$ mice displayed behavioral abnormality and early postnatal death was never observed.

3.3. Homozygous mutant mice show abnormal EEG and EMG activity

To quantify the phenotype of tremors and seizures in *asc-1*$^{-/-}$ mice, standard EEG and EMG recordings were performed on the few *asc-1*$^{-/-}$ mice that did survive until 30–35 days old (n = 3) and WT mice (n = 6). When *asc-1*$^{-/-}$ mice did not display behavioral tremors and seizures, both

EEG and EMG signals and corresponding spectra during wakefulness, rapid-eye-movement (REM) sleep, and non-REM sleep appeared normally (Fig. 3) and exhibited the typical patterns characteristic for WT mice [4]. When paroxysmal behavioral abnormalities occurred, the EEG and EMG recordings confirmed the observed behavioral tonic–clonic, seizure-like activity and tremors. Interestingly, the tonic–clonic activity comprised of high amplitude and frequency of muscle contractions detected by the EMG, was, however, rarely associated with abnormalities in the EEG. Over a 24-h recording period, 1302 instances of clonic–tonic EMG events were counted of which only 6% were accompanied with EEG seizure-like activity (Fig. 4A). Conversely, of the 187 EEG seizure-like events observed over this period, approximately 41% of the EEG seizure event was accompanied by EMG abnormal activity (Fig. 4B). Furthermore, the EMG recordings confirmed the presence of long-lasting tremor activity that was usually triggered by one or two brief tonic–clonic EMG events (Fig. 4C). The tremors were regular and of lower amplitude compared to tonic–clonic EMG activity, with frequencies around 7–15 Hz (Fig. 4D). During tremors, EEG signals appeared normal and were typical of that during wakefulness (Figs. 4C, D; compare with Fig. 3 in which traces of the same individual are depicted). However, when there was a generalized behavioral seizure, the EEG recording revealed paroxysmal activity characterized by pronounced '40-Hz' frequency activity (25–55 Hz), associated with EMG abnormality that could last up to 30 s (Figs. 4E and F). The other two *asc-1*$^{-/-}$ mice recorded displayed very similar EEG/EMG abnormalities, whereas in none of the WT controls such abnormal activities were observed. All three *asc-1*$^{-/-}$ mice recorded by EEG and EMG eventually died between postnatal days 36 and 40 following severe seizures as indicated by a dramatic increase in the '40-Hz' EEG events on the day before death.

3.4. Homozygous mutant mice show abnormal synaptic activity in hippocampal slices

In an attempt to investigate the apparent hyperexcitable phenotype of *asc-1*$^{-/-}$ at the cellular level, we examined neuronal synaptic activity in the hippocampus, a brain region which has high NMDA receptor density and moderate Asc-1 expression ([11,14], though the *lacZ* expression is low, see Fig. 1C) and is prone to generation of seizure activity in vivo as well as in vitro preparations. Extracellular recordings were conducted in hippocampal slices taken from WT and *asc-1*$^{-/-}$ mouse brains. In artificial cerebrospinal fluid (ACSF) containing 2 mM Mg^{2+}, no spontaneous or evoked seizure-like activity were observed. Unexpectedly, the amplitude of evoked EPSPs and population spikes (PS) in the CA1 region were smaller in *asc-1*$^{-/-}$ compared to WT slices. Mean fiber potential (FP) amplitude and EPSP slope values across input/output (I/O) curves were decreased in stratum radiatum recordings in *asc-1*$^{-/-}$ compared to WT slices (Figs. 5A and B). There were, however, no significant differences in EPSP/FP ratios between *asc-1*$^{-/-}$ and WT mice, indicating similar synaptic strength (Fig. 5C). Moreover, PS amplitude recorded in stratum pyramidale was also smaller for *asc-1*$^{-/-}$ slices across the I/O curve (Figs. 5D and E). In contrast, when Mg^{2+} was omitted from the ACSF to remove Mg^{2+} inhibition of NMDA receptors, PS amplitude increased significantly more for the *asc-1*$^{-/-}$ slices than WT slices suggesting a greater sensitivity to nominal Mg^{2+}-free conditions in the absence of the Asc-1 transporter (Fig. 5F).

4. Discussion

We have demonstrated that target-directed deletion of the *asc-1* gene resulted in tremors and seizures in homozygous KO mice, which severely impaired movement and caused early postnatal death. These findings suggest that Asc-1 plays an essential physiological role in regulation of neuronal excitability.

The expression pattern of the *lacZ* reporter in the CNS of *asc-1*$^{+/-}$ mice are, in general, consistent with studies [11,14] with the exception of the low level of expression in various forebrain areas (Fig. 1B). This discrepancy is not easily explained but may have resulted from differences in the two methodologies employed; one directly detects Asc-1 protein distribution whereas the other assesses *lacZ* expression initiated from the *asc-1* promotor. Interestingly, in the spinal cord, *lacZ* staining was found in gray matter exclusively, which underscores that, as in the brain [11,14], *asc-1* is strictly expressed in neuronal structures.

The null *asc-1*$^{-/-}$ mice gradually developed periodic spontaneous seizures and tremors around 20 days of age. EEG and EMG recordings not only quantified the observed tonic–clonic, seizure-like behavior, and tremors in *asc-1*$^{-/-}$ mice, but also suggest the involvement of sub-cerebral electrical discharges as the origin of the tonic–clonic muscle contractions and seizures. The tonic–clonic muscle contractions resemble a condition referred to as myoclonus, which may arise from deep brain structures and the spinal cord [19] where the *lacZ* reporter gene was abundantly expressed. Simultaneous recordings of sub-cerebral neuronal activity or spinal motorneuron activity and EMG in *asc-1*$^{-/-}$ mice could further identify the origin of the myoclonus and tremors.

Also, the in vitro extracellular recordings indicate that the hippocampus was not a focus triggering behavioral seizures, as no signs of spontaneous or evoked seizure activity in the hippocampal CA1 area were observed in the *asc-1*$^{-/-}$ hippocampal slices. Unexpectedly, a clear reduction in several baseline electrophysiological parameters (e.g., EPSPs and population spikes) was observed in KO compared to WT hippocampal slices. These phenomena could have resulted from multiple factors. For example,

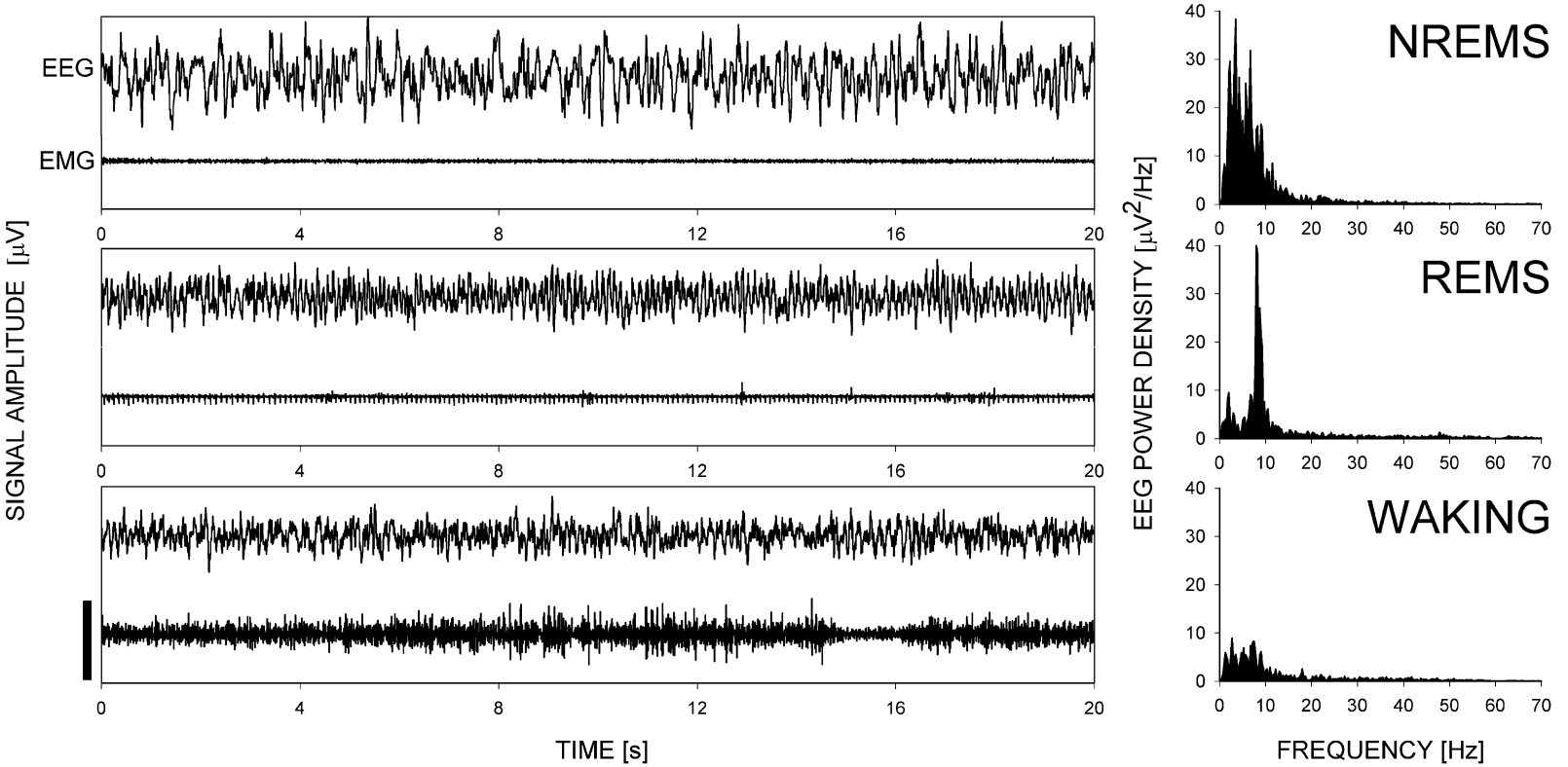

Fig. 3. Representative examples of EEG and EMG signals (left panels) and corresponding EEG spectra (right panels) of one *asc-1*$^{-/-}$ mouse, when seizures or tremors were absent. Normal EEG activity was observed during non-REM sleep [NREMS; high-amplitude EEG with slow-wave oscillations in the delta frequency range (1.0–4.5 Hz); low EMG; upper panels], REM sleep (REMS: regular theta rhythm in EEG; muscle atonia; middle panels; note heartbeat in EMG signal), and wakefulness (low-amplitude, mixed frequency EEG; high EMG). All EEG/EMG samples were taken from the same mouse recorded continuously for 5 days. EEG and EMG amplitudes were plotted at the same scale (scale bar: 400 μV).

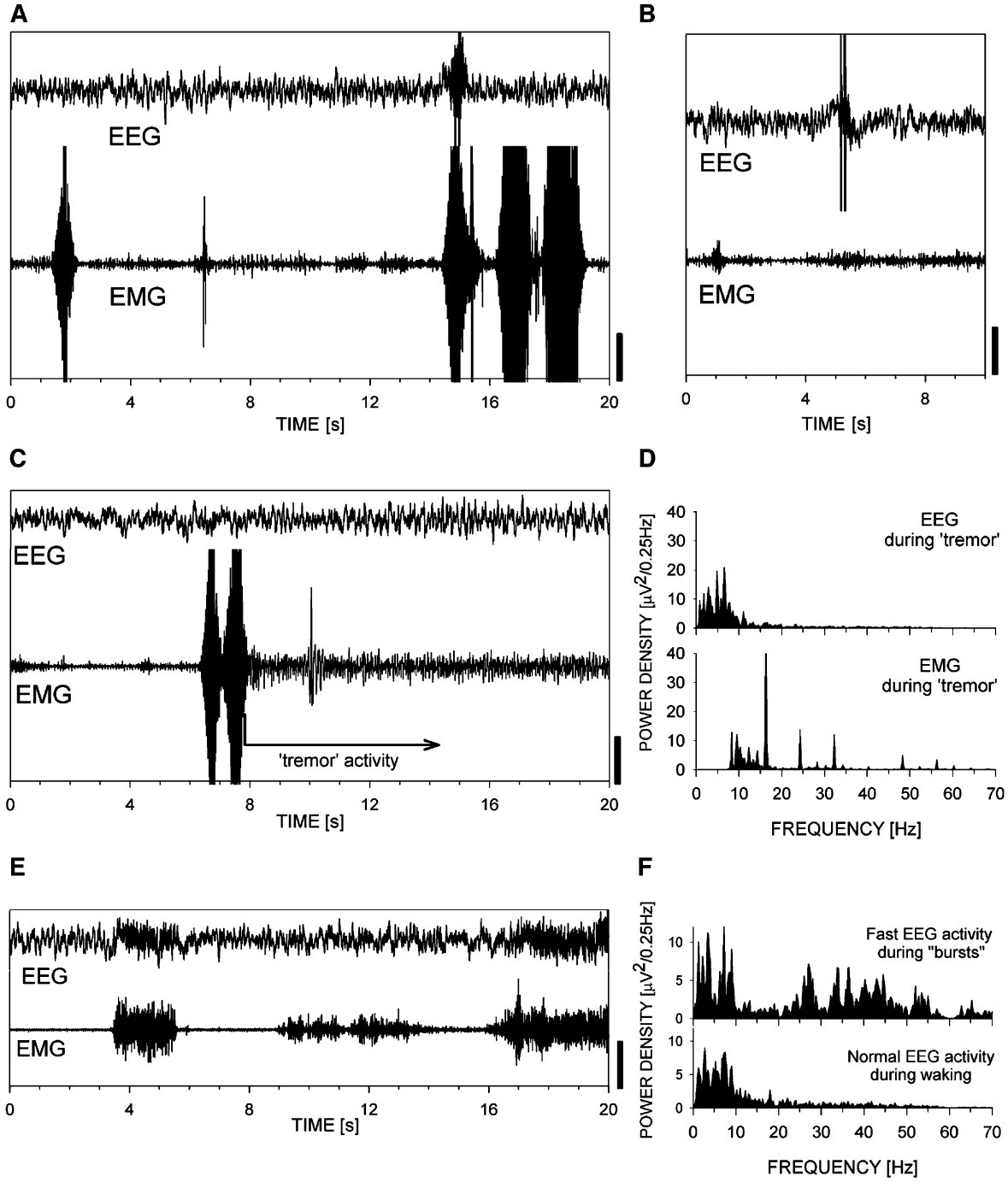

Fig. 4. Representative examples of paroxysmal EEG and EMG activity (same individual as in Fig. 3) (A) *asc-1*$^{-/-}$ mice displayed tonic–clonic EMG activity during wakefulness that was only rarely accompanied by seizure-like EEG activity. (B) Approximately 60% of the seizure-like EEG activity was not associated with paroxysmal EMG events. (C) Highly regular tremor activity was usually initiated by sudden, brief tonic–clonic EMG activity, while the EEG was apparently normal. (D) Spectral analysis revealed a profound peak in the 7–15 Hz range in the EMG signal during tremors. (E) Paroxysmal bursts of low-amplitude, fast ('40-Hz') EEG activity were always associated with tonically increased EMG activity. (F) EEG activity was increased dramatically in the (25–55 Hz) range. This mouse died at 40 days of age following a prolonged and intensive burst of '40-Hz' EEG activity (not shown). EEG and EMG amplitudes were plotted at the same scale in panels A–C, and E (scale bars: 400 μV).

poor development of pyramidal neurons could be due to a reduced intracellular L-serine supply, since L-serine is also transported by Asc-1 and is essential for survival and development of neurons [6]. Alternatively, this reduction could have resulted from chronically recurrent seizure-induced cell loss as was observed in many experimental epileptic models, such as the kainic acid-induced seizure model [12].

Under nominal Mg^{2+}-free conditions, a relatively greater increase in evoked synaptic responses was

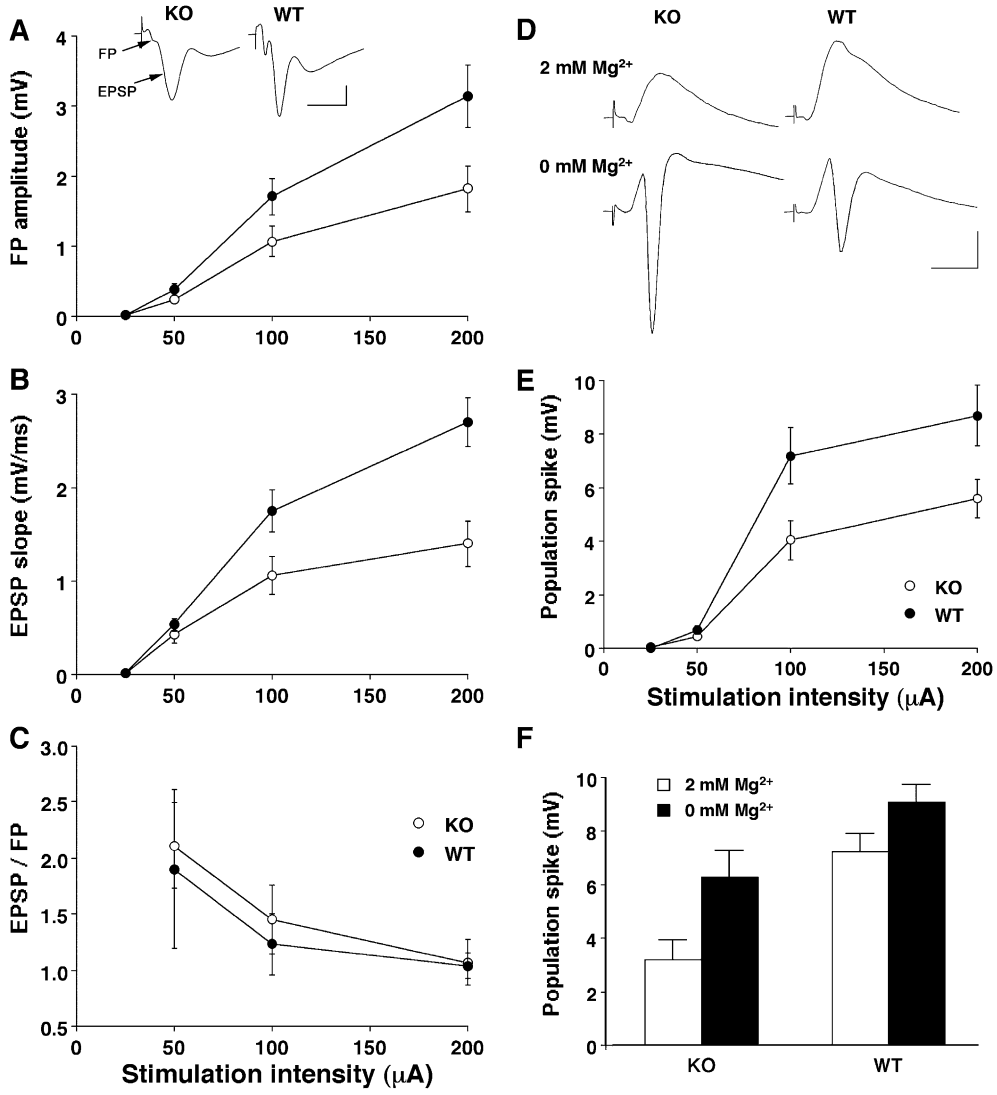

Fig. 5. (A–C) Schaffer collateral field potential (FP) and CA3–CA1 field EPSP slope are reduced in *asc-1*$^{-/-}$ slices whereas synaptic strength (EPSP/FP) in the stratum radiatum remains unaltered. (A) Mean FP amplitude ($F_{1,66} = 4.98$, $P < 0.05$) and (B) EPSP slopes ($F_{1,66} = 7.59$, $P < 0.01$) across input/output (I/O) curves were decreased in a*sc-1*$^{-/-}$ slices (KO; open circles, $n = 17$) compared to wild-type (WT; filled circles, $n = 18$). Inset in panel A shows averaged waveforms (5 sweeps) of responses evoked by electric stimulation (100 μA, 100 μs; scale bars: 0.5 mV, 10 ms). (C) EPSP/FP ratios, calculated for responses above threshold, did not differ between genotypic groups indicating similar synaptic strengths. (D–F) The mean population spike (PS) recorded across I/O curves is reduced but the excitability response to Mg^{2+} removal is enhanced in *asc-1*$^{-/-}$ compared to WT slices. (D) Averaged waveforms (5 sweeps) representing evoked responses (50 μA stimulation intensity) recorded in stratum pyramidale in 2 (top) or 0 mM Mg^{2+} (bottom; scale bars: 2 mV, 10 ms). (E) PS amplitude was smaller for *asc-1*$^{-/-}$ slices in standard ACSF containing 2 mM Mg^{2+} ($F_{1,66} = 5.49$, $P < 0.05$). (F) Summary histograms comparing PS amplitude (evoked by 50 μA stimulation intensity) for KO and WT slices superfused with 2 or 0 mM Mg^{2+}. After Mg^{2+} removal, PS relatively increased more for KO than for WT slices, indicating greater sensitivity to Mg^{2+} removal in *asc-1*$^{-/-}$ slices ($F_{1,58} = 6.87$, $P < 0.02$).

observed in the *asc-1*$^{-/-}$ hippocampal slices compared to WT. Our previous studies showed that population spikes recorded under nominal Mg^{2+}-free conditions were substantially depressed by the NMDA receptor antagonist, 2-amino-5-phosphonopentanoic acid, confirming that they were principally mediated by NMDA receptor-mediated synaptic responses [24]. Because D-serine is a co-agonist acting on the glycine site of the NMDA receptor, this relatively increased synaptic responses in *asc-1*$^{-/-}$ slices is likely to have resulted from an enhancement of NMDA receptor activation presumably resulting from accumulated extracellular D-serine. This is supported by the in vivo experiment described above, in which the NMDA receptor antagonist MK-801 reduced hyperexcitability in *asc-1*$^{-/-}$ mice.

Amino-acid transport across cellular membranes is mediated by multiple transporters with overlapping specificities. In particular, Asc-1 also has a high affinity for glycine (K_i: 9–13 μM) [11]. Therefore, in addition to D-serine, extracellular levels of glycine could also have been affected by the Asc-1 deletion and, consequently, might have contributed to the hyperexcitability observed in *asc-1*$^{-/-}$ mice. However, because other, more specific glycine transporters exist (e.g., GlyT-1 and -2), extracellular glycine levels in *asc-1*$^{-/-}$ mice are expected to be affected to a

lesser extent as compared to D-serine levels for which no other high-affinity transporters have been identified so far. Moreover, the phenotype of mice lacking these specific glycine transporters differs from that observed in *asc-1*$^{-/-}$ mice; GlyT-1 null mice die within 12 h of birth [20], while GlyT-2-deficient mice develop a lethal neuromotor deficiency during postnatal week two [7]. Interestingly, the gene targeted knockouts of the Na^+-dependent large neutral amino-acid transporter-1 (*Slc7a7*) and the cystine–glutamate exchange transporter (*Slc7a11*) did not cause tremors or seizures (unpublished observations, Xie et al., at Deltagen Inc.). Together, these findings underline that the phenotype described here in *asc-1*$^{-/-}$ mice does not extend to other, similar amino-acid transporters, and is likely to be related to its specificity for D-serine. Obviously, a causal relationship between elevated D-serine concentrations and the occurrence of seizures and tremors should be established more definitively in future studies by directly measuring extracellular D-serine levels in *asc-1*$^{-/-}$ mice.

Taken together with the known neurochemical properties and neuronal specific distribution of the Asc-1 transporter [8,9,11,14], the present functional study implicates that the mechanism underlying the behavioral hyperexcitability in mutant mice is likely due to overactivation of NMDA receptors, presumably resulting from accumulated extracellular D-serine. Our initial characterization of the Asc-1 transporter in the CNS function and behavior provides the first evidence to support the notion that Asc-1 transporter plays a critical role in regulating neuronal excitability, and indicates that the transporter is vital to postnatal survival of mice.

Acknowledgments

Dr. Xie was a Visiting Scholar at the Department of Biological Sciences, Stanford University. This research was supported in part by NIH Grants HL64148, R43-RR017182, and R43-MH07162.

References

[1] J.L. Arriza, M.P. Kavanaugh, W.A. Fairman, Y.N. Wu, G.H. Murdoch, R.A. North, S.G. Amara, Cloning and expression of a human neutral amino acid transporter with structural similarity to the glutamate transporter gene family, J. Biol. Chem. 268 (1993) 15329–15332.
[2] A. Chairoungdua, Y. Kanai, H. Matsuo, J. Inatomi, D.K. Kim, H. Endou, Identification and characterization of a novel member of the heterodimeric amino acid transporter family presumed to be associated with an unknown heavy chain, J. Biol. Chem. 276 (2001) 49390–49399.
[3] J.N. Crawley, Exploratory behavior models of anxiety in mice, Neurosci. Biobehav. Rev. 9 (1985) 37–44.
[4] P. Franken, A. Malafosse, M. Tafti, Genetic variation in EEG activity during sleep in inbred mice, Am. J. Physiol. 275 (1998) R1127–R1137.
[5] Y. Fukasawa, H. Segawa, J.Y. Kim, A. Chairoungdua, D.K. Kim, H. Matsuo, S.H. Cha, H. Endou, Y. Kanai, Identification and characterization of a Na(+)-independent neutral amino acid transporter that associates with the 4F2 heavy chain and exhibits substrate selectivity for small neutral D- and L-amino acids, J. Biol. Chem. 275 (2000) 9690–9698.
[6] S. Furuya, T. Tabata, J. Mitoma, K. Yamada, M. Yamasaki, A. Makino, T. Yamamoto, M. Watanabe, M. Kano, Y. Hirabayashi, L-Serine and glycine serve as major astroglia-derived trophic factors for cerebellar Purkinje neurons, Proc. Natl. Acad. Sci. U. S. A. 97 (2000) 11528–11533.
[7] J. Gomeza, K. Ohno, S. Hulsmann, W. Armsen, V. Eulenburg, D.W. Richter, B. Laube, H. Betz, Deletion of the mouse glycine transporter 2 results in a hyperekplexia phenotype and postnatal lethality, Neuron 40 (2003) 797–806.
[8] A. Hashimoto, T. Oka, Endogenous free D-aspartate and D-serine in mammals, Seikagaku 68 (1996) 1458–1462.
[9] A. Hashimoto, T. Oka, Free D-aspartate and D-serine in the mammalian brain and periphery, Prog. Neurobiol. 52 (1997) 325–353.
[10] A. Hashimoto, T. Oka, T. Nishikawa, Extracellular concentration of endogenous free D-serine in the rat brain as revealed by in vivo microdialysis, Neuroscience 66 (1995) 635–643.
[11] L. Helboe, J. Egebjerg, M. Moller, C. Thomsen, Distribution and pharmacology of alanine–serine–cysteine transporter 1 (asc-1) in rodent brain, Eur. J. Neurosci. 18 (2003) 2227–2238.
[12] J.P. Leite, N. Garcia-Cairasco, E.A. Cavalheiro, New insights from the use of pilocarpine and kainate models, Epilepsy Res. 50 (2002) 93–103.
[13] T. Matsui, M. Sekiguchi, A. Hashimoto, U. Tomita, T. Nishikawa, K. Wada, Functional comparison of D-serine and glycine in rodents: the effect on cloned NMDA receptors and the extracellular concentration, J. Neurochem. 65 (1995) 454–458.
[14] H. Matsuo, Y. Kanai, M. Tokunaga, T. Nakata, A. Chairoungdua, H. Ishimine, S. Tsukada, H. Ooigawa, H. Nawashiro, Y. Kobayashi, J. Fukuda, H. Endou, High affinity D- and L-serine transporter Asc-1: cloning and dendritic localization in the rat cerebral and cerebellar cortices, Neurosci. Lett. 358 (2004) 123–126.
[15] B.S. Meldrum, Glutamate as a neurotransmitter in the brain: review of physiology and pathology, J. Nutr. 130 (2000) 1007S–1015S.
[16] J. Nakauchi, H. Matsuo, D.K. Kim, A. Goto, A. Chairoungdua, S.H. Cha, J. Inatomi, Y. Shiokawa, K. Yamaguchi, I. Saito, H. Endou, Y. Kanai, Cloning and characterization of a human brain Na(+)-independent transporter for small neutral amino acids that transports D-serine with high affinity, Neurosci. Lett. 287 (2000) 231–235.
[17] N.F. Ruby, T.J. Brennan, X. Xie, V. Cao, P. Franken, H.C. Heller, B.F. O'Hara, Role of melanopsin in circadian responses to light, Science 298 (2002) 2211–2213.
[18] M.J. Schell, M.E. Molliver, S.H. Snyder, D-Serine, an endogenous synaptic modulator: localization to astrocytes and glutamate-stimulated release, Proc. Natl. Acad. Sci. U. S. A. 92 (1995) 3948–3952.
[19] E. Shivapour, R.D. Teasdall, Spinal myoclonus with vacuolar degeneration of anterior horn cells, Arch. Neurol. 37 (1980) 451–453.
[20] G. Tsai, R.J. Ralph-Williams, M. Martina, R. Bergeron, J. Berger-Sweeney, K.S. Dunham, Z. Jiang, S.B. Caine, J.T. Coyle, Gene knockout of glycine transporter 1: characterization of the behavioral phenotype, Proc. Natl. Acad. Sci. U. S. A. 101 (2004) 8485–8490.
[21] N. Utsunomiya-Tate, H. Endou, Y. Kanai, Cloning and functional characterization of a system ASC-like Na+-dependent neutral amino acid transporter, J. Biol. Chem. 271 (1996) 14883–14890.
[22] H. Wolosker, S. Blackshaw, S.H. Snyder, Serine racemase: a glial enzyme synthesizing D-serine to regulate glutamate-*N*-methyl-D-aspartate neurotransmission, Proc. Natl. Acad. Sci. U. S. A. 96 (1999) 13409–13414.

[23] H. Wolosker, R. Panizzutti, J. De Miranda, Neurobiology through the looking-glass: D-serine as a new glial-derived transmitter, Neurochem. Int. 41 (2002) 327–332.
[24] X. Xie, T.G. Smart, Modulation of long-term potentiation in rat hippocampal pyramidal neurons by zinc, Pflugers Arch. 427 (1994) 481–486.
[25] X. Xie, T. Dumas, L. Tang, T. Brennan, T. Reeder, J.E. Flores-Mercado, B.F. O'Hara, P. Franken, A physiological role for asc-1 neutral amino acid-transporter in the CNS studied by gene knockout in mice, Abstr. - Soc. Neurosci. (2003) 688.11.
[26] T. Yamamoto, I. Nishizaki, S. Furuya, Y. Hirabayashi, K. Takahashi, S. Okuyama, H. Yamamoto, Characterization of rapid and high-affinity uptake of L-serine in neurons and astrocytes in primary culture, FEBS Lett. 548 (2003) 69–73.